J. Fluid Mech. (1970), *vol.* 43, *part* 1, *pp.* 49–75
Printed in Great Britain

On stagnation-point conditions in non-equilibrium inviscid blunt-body flows

By MARCEL VINOKUR
Lockheed Palo Alto Research Laboratory, Palo Alto, California

(Received 31 October 1969)

In non-equilibrium inviscid blunt-body flows, the state of the gas at the stagnation point is known to be in thermodynamic equilibrium for all finite relaxation times. The dependence of this state on the non-equilibrium processes and body geometry is investigated for the most general conditions. The stagnation-point state is always found to be in a narrow range bounded on one side by the state obtained in an equilibrium flow. The other bound, called the frozen limit, is far removed from the state obtained in an identically frozen flow (infinite relaxation times). For certain state variables, the frozen-limit value lies outside the range determined by frozen and equilibrium flow. Significant errors are found in several published predictions of the stagnation-point state, resulting from the non-analytic approach to equilibrium in nearly frozen flow.

The two bounds on the pressure are expressible in terms of the normal shock density ratios for equilibrium and frozen flow. The actual pressure for an arbitrary flow situation is found to depend only on the shock nose radius and the relation between density and time in the relaxation zone behind a normal shock wave. If the density law is given by a single relaxation model, a closed form expression for the pressure is obtained. The analysis is carried out for both plane and axisymmetric flows, and is also valid for non-equilibrium free-stream conditions.

1. Introduction

Among the many difficulties that beset the inviscid supersonic blunt-body problem, there is at least one saving grace. For the symmetric flow of a gas in equilibrium, the stagnation-point state is uniquely defined by the free-stream conditions. This information plays an important role in the direct methods of approach in which the body is specified. In the indirect methods, in which the shock wave is specified, the known stagnation-point state serves as a useful check on the accuracy of the solution.

The situation for non-equilibrium flow is not entirely clear. The stagnation-point enthalpy is clearly equal to the total enthalpy in the free stream, but there remains the question whether other state variables depend on the non-equilibrium processes and the body shape. While there has been a considerable body of literature on non-equilibrium blunt-body flows since the pioneering work of Freeman (1958), there is still considerable confusion concerning this question. Some

investigators have assumed that the stagnation-point state is independent of the degree of non-equilibrium, while others have reported a strong dependence for certain state variables. The resolution of this discrepancy is the main purpose of the present work.

For bodies with smooth nose shapes, most investigators have either stated or deduced that the gas is always in thermodynamic equilibrium at the stagnation point (for finite relaxation times). While this fact may be intuitively obvious, a rigorous proof was lacking, since the analytic solutions were based on certain approximations, and the purely numerical schemes were limited in accuracy. Recently, independent investigations by Stulov & Turchak (1966) for vibrational relaxation, and Conti & Van Dyke (1966, 1969*a*) for dissociation of a Lighthill gas, established rigorously by means of a local analysis that equilibrium conditions are in fact reached at the stagnation point. (One should note that the analysis of Stulov & Turchak is not completely correct, as will be indicated later.) They also showed that certain state variables could approach the stagnation point along the axis with infinite gradients. Although these analyses could not determine the variation of this equilibrium state itself with changes in the non-equilibrium parameters, they made evident why such discrepancies could exist concerning this question.

In what follows, the basic equations will be formulated, and previous analyses that bear on the question of the stagnation-point state will be critically reviewed. After presenting some generalizations of the results of the local analyses referred to above, we will show how the variation of this state with the non-equilibrium process can be simply predicted. Both plane and axisymmetric flows will be simultaneously treated, and the effect of a non-equilibrium free stream will be included.

2. Formulation of the problem

We consider the steady, symmetric (plane or axisymmetric) flow due to a blunt-nosed body immersed in a uniform, supersonic stream. Translational equilibrium is assumed to exist among the molecular species, thus defining a translational temperature at every point. Molecular transport is neglected, so that the detached shock wave becomes a discontinuous surface. Non-adiabatic processes such as energy loss due to radiation are assumed absent.

We will use a Cartesian or cylindrical co-ordinate system, with origin at the stagnation point, as shown in figure 1. The shock position on the axis is at $y = \delta$. The shock nose radius R_s, free-stream velocity U_∞ and free-stream density ρ_∞ will serve as reference quantities. The conservation equations for our model are

mass: $$(\rho x^j u)_x + x^j(\rho v)_y = 0; \tag{1a}$$

x momentum: $$uu_x + vu_y + p_x/\rho = 0; \tag{1b}$$

y momentum: $$uv_x + vv_y + p_y/\rho = 0; \tag{1c}$$

energy: $$h + \tfrac{1}{2}(u^2 + v^2) = h_\infty + \tfrac{1}{2}U_\infty^2; \tag{1d}$$

where u, v are velocity components in the x, y directions, and ρ, p, h refer to the density, pressure, and specific enthalpy. Subscripts x, y indicate partial differentiation, while the index $j = 0$ for plane flow, and $j = 1$ for axisymmetric flow.

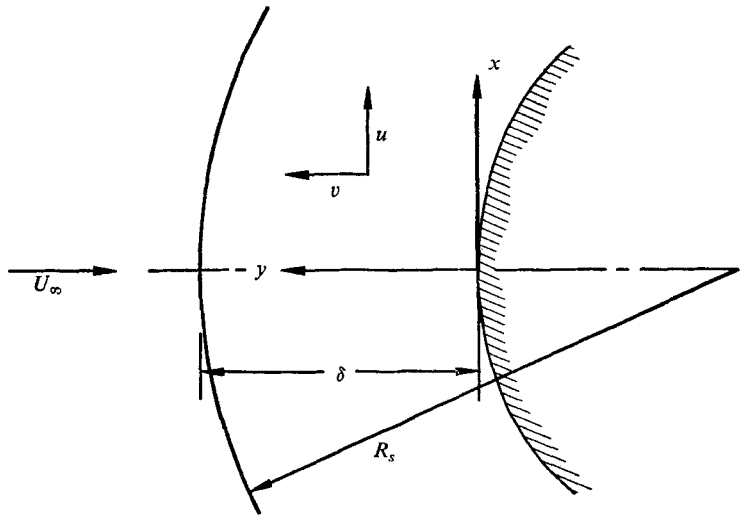

FIGURE 1. Co-ordinate system.

Generalizing the nomenclature of Vincenti & Kruger (1965), we assume that the thermodynamic state of the gas is determined by specifying the independent variables p, h and n general non-equilibrium variables $q_1, q_2, \ldots, q_n$. Some q_i can represent the specific energy of the rotational, vibrational, or electronic state of a species, while others represent the concentration or mass fraction of one of several species. A q_i could also refer to the electron temperature. The q_i chosen are those that are sensibly out of equilibrium in some part of the flow, and that give a non-negligible contribution to the determination of ρ. Admittedly, this choice can only be made *a posteriori* in some situations.

In addition to the density ρ, we will subsequently introduce the specific entropy S, the temperature T and the frozen sound speed a_f. These are given by equations of state of the form

$$\rho = \rho(p, h, q_1, q_2, \ldots, q_n), \tag{2a}$$

$$S = S(p, h, q_1, q_2, \ldots, q_n), \tag{2b}$$

$$T = T(p, h, q_1, q_2, \ldots, q_n), \tag{2c}$$

and

$$a_f = a_f(p, h, q_1, q_2, \ldots, q_n). \tag{2d}$$

Equations (2) are not independent, but are related through the first and second laws of thermodynamics by

$$\left(\frac{\partial S}{\partial p}\right)_{h,q_i} = -\frac{1}{\rho T}, \quad \left(\frac{\partial S}{\partial h}\right)_{p,q_i} = \frac{1}{T}, \tag{3a}$$

and

$$a_f^{-2} \equiv \left(\frac{\partial \rho}{\partial p}\right)_{S,q_i} = \frac{1}{\rho}\left(\frac{\partial \rho}{\partial h}\right)_{p,q_i} + \left(\frac{\partial \rho}{\partial p}\right)_{h,q_i}. \tag{3b}$$

The non-equilibrium processes are assumed to be governed by m coupled reactions, (the word 'reaction' is used to describe dissociation-recombination,

ionization, vibrational relaxation, etc.) each of which involves some of the variables q_i. The rate of change of the variable q_i due to reaction r is given by the generalized rate equation

$$\left(\frac{Dq_i}{Dt}\right)_r \equiv \left(u\frac{\partial q_i}{\partial x}+v\frac{\partial q_i}{\partial y}\right)_r = \omega_{i,r}(p,h,q_1,q_2,\ldots,q_n). \tag{4}$$

The function $\omega_{i,r}$ can also be written in terms of the local relaxation time $\tau_{i,r}$ as

$$\omega_{i,r} = \frac{\chi_{i,r}(p,h,q_1,q_2,\ldots,q_n)}{\tau_{i,r}(p,h,q_1,q_2,\ldots,q_n)}. \tag{5}$$

The total rate of change of q_i due to all reactions is then given by

$$\frac{Dq_i}{Dt} = \sum_{r=1}^{m} \omega_{i,r}. \tag{6}$$

Under the condition of complete thermodynamic equilibrium, the thermodynamic state of the gas can be considered a function of p and h only. From statistical mechanics, the variables q_i are then determined by relations of the form

$$q_i = q_i^*(p,h) \tag{7}$$

at equilibrium. Substitution of (7) into equations (2) yields equilibrium relations for other state variables, e.g.

$$\rho^*(p,h) = \rho[p,h,q_1^*(p,h),q_2^*(p,h),\ldots,q_n^*(p,h)], \text{ etc.} \tag{8}$$

Since $\omega_{i,r} = 0$ at equilibrium for all i and r, it follows that the functions $\chi_{i,r}$ must satisfy the condition

$$\chi_{i,r}(p,h,q_1^*,q_2^*,\ldots,q_n^*) = 0 \tag{9}$$

for all i and r. The local relaxation times $\tau_{i,r}$, on the other hand, take on finite *non-zero* values under all physically realizable conditions. The conditions $\tau_{i,r} = 0$ (equilibrium flow) and $\tau_{i,r} = \infty$ (frozen flow) for all i and r can only be approached as mathematical limits, which may be non-uniform under certain situations. This point will be discussed further in § 5.

The condition of complete thermodynamic equilibrium is approached asymptotically in certain well-known non-equilibrium steady flows. One such case is that of an isobaric flow, i.e. a flow at constant pressure. From momentum and energy considerations it follows that the velocity and the specific enthalpy are constant. The temporal evolution of each q_i is thus obtained by integration of the set of equations (4) to (6), with p and h held constant. Since distance is proportional to the time, the solution also gives the spatial evolution of the q_i. In the limit of infinite time or distance, each q_i must approach the equilibrium value given by (7), irrespective of its initial value. This solution is just the Galilean transformation of that for a closed, adiabatic system, which is assumed to be inherently stable.

A more interesting case is a strictly one-dimensional flow, such as exists in the relaxation zone behind a normal shock wave. If v is the one-dimensional velocity

(positive in the upstream direction), the equations in the relaxation zone, obtained by integrating equations (1), can be written as

$$\rho v = -\rho_\infty U_\infty, \tag{10a}$$

$$p+\rho v^2 = p_\infty+\rho_\infty U_\infty^2, \tag{10b}$$

$$h+\tfrac{1}{2}v^2 = h_\infty+\tfrac{1}{2}U_\infty^2. \tag{10c}$$

Since the shock wave is assumed to be of zero thickness, the non-equilibrium variables immediately behind the shock wave assume their upstream values. Therefore

$$q_{is} = q_{i\infty}. \tag{11}$$

The other state variables behind the shock wave are obtained by the simultaneous solution of (2), (10) and (11). Using these as initial conditions, equations (2), (10), and the one-dimensional rate equation,

$$v\frac{dq_i}{dy} = \sum_{r=1}^{m}\omega_{i,r}, \tag{12}$$

can be integrated to determine the solution in the relaxation zone. In the limit of infinite distance downstream of the shock wave, the state of the gas will approach the equilibrium state given by the simultaneous solution of (8*a*) and (10). This state is also the state immediately behind the shock wave for the singular equilibrium flow conditions $\tau_{i,r} = 0$.

In the present problem, the conditions on the axis behind the shock wave are identical to the frozen conditions behind a normal shock wave. But the flow near the axis of symmetry is two-dimensional. Specializing equations (1) in the vicinity of the axis, where

$$u \approx xu_x \quad \text{and} \quad p_x \approx xp_{xx},$$

we obtain the following set of equations, valid on the axial streamline:

$$\frac{d}{dy}(\rho v)+(1+j)\rho u_x = 0, \tag{13a}$$

$$u_x^2+v\frac{du_x}{dy} = -\frac{1}{\rho}p_{xx}, \tag{13b}$$

$$v\frac{dv}{dy} = -\frac{1}{\rho}\frac{dp}{dy}, \tag{13c}$$

$$h+\tfrac{1}{2}v^2 = h_\infty+\tfrac{1}{2}U_\infty^2. \tag{13d}$$

The presence of p_{xx} in (13*b*) makes the system (2*a*), (12) and (13) incomplete, attesting to the basic elliptic nature of the subsonic flow. Thus, the integration of the flow along the axial streamline in order to obtain the stagnation-point state cannot be accomplished without some additional assumptions or approximations. In the next section we will examine the various approximations employed by previous investigators to solve equations (13), as well as the results of numerical solutions of the full equations (1). In some of the discussion, it will be convenient to introduce the Lagrange particle time t, related to the velocity v and position y by

$$v = Dy/Dt. \tag{14}$$

3. Review of previous analyses

Semi-analytic solutions

We now present a unified discussion of previous semi-analytic treatments of non-equilibrium blunt-body flows, confining our attention to the determination of the stagnation-point conditions. Although some of the investigators employed spherical or cylindrical co-ordinates referred to the body or to the shock wave, our discussion will be based on equations (13). Thus, some of the relations we present will differ in detail from the actual ones employed due to the absence of curvature terms.

The various solutions can be classified in several different ways. While some investigators employed the transverse momentum equation (13*b*), approximating p_{xx} in some manner, others discarded it entirely and chose instead an approximate form of the normal momentum equation (13*c*). A different kind of grouping is that between those who solved the coupled set of equations (2*a*), (12) and (13), and those who attempted to uncouple the non-equilibrium processes from the fluid mechanics. The latter employed a mapping technique to map a previously determined isobaric or normal shock solution (discussed in the previous section) onto the axial streamline. The mapping function in each case was determined by simple integrations.

The earliest semi-analytic treatment is found in Freeman's (1958) paper.† He employed the Newtonian approximation to solve for the flow of Lighthill's ideal dissociating gas past a sphere. The non-equilibrium variable q is identified with the atom mass fraction α. Freeman introduced a new independent variable Θ along each streamline defined by

$$\Theta = C \int_0^t \frac{p}{h}\, dt, \tag{15}$$

where t is the Lagrange particle time measured from the shock wave, and C is a proportionality constant in his assumed rate law. According to the Newtonian approximation, the specific enthalpy on each streamline is a constant. Furthermore, on the axis, where there is no centrifugal correction, the Newtonian pressure behind the shock wave is impressed directly on the body. Therefore Θ is just proportional to t on the axial streamline. Using the strong-shock values $p = \rho_\infty U_\infty^2$ and $h = \frac{1}{2}U_\infty^2$, Freeman numerically integrated the rate equation (12), with the aid of (14) and (15), to obtain the isobaric solution $\alpha(\Theta)$. Substitution into (2*a*) then yielded $\rho(\Theta)$. The mapping from Θ to y is accomplished from the inversion of (14), which can be written as

$$\delta - y = -\int_0^t \frac{\rho v}{\rho}\, dt. \tag{16}$$

The dependence of ρv on t (or Θ) was obtained from (13*a*), (13*b*) and (14), neglecting the term $(1/\rho)p_{xx}$ in (13*b*). While this approximation, based on the condition $\rho/\rho_\infty \gg 1$, is valid behind the shock wave, it must break down at the

† The following interpretation of Freeman's work differs somewhat from the presentation in his original paper, and is motivated by Chisnell (1966).

stagnation point, where $v = 0$ and $p_{xx} \neq 0$. The function $\rho v(t)$ is a simple closed form expression that will be derived in § 6.

The results of Freeman's analysis are embodied in his figure 9, which shows the variation of α from the shock wave to the body for different values of a dimensionless relaxation time. The curves exhibit the proper qualitative behaviour of a gradual approach to the stagnation-point value for small relaxation times, and steep gradients for large relaxation times. The final conclusion that the same equilibrium state is reached for all finite relaxation times is subject to question, since it rests on the assumption of an isobaric process, which is not strictly correct. Also, gradients near the stagnation point are in error, due to the improper treatment of (13*b*).

A similar analysis was carried out by Murzinov (1961) for vibrational relaxation. He also assumed a constant pressure (taken to be the average of the pressure at the body and the shock for *frozen* flow) and constant enthalpy (equal to the stagnation enthalpy). The variable q is the vibrational energy E_v. Murzinov introduced the Howarth–Dorodnitsyn variable

$$\eta = \frac{1}{\rho_s}\int_0^y \rho\, dy \tag{17}$$

as his new independent variable. Since the right-hand side of (13*b*) is important only near the body, he approximated it by its stagnation-point value, i.e. $(1/\rho)p_{xx} = -u_{xb}^2$, where the subscript b refers to quantities evaluated at the body. Equations (13*a*) and (13*b*) then yielded a closed form expression for $\rho v(\eta)$, which was used to obtain $E_v(\eta)$ by integrating (12), and finally $\rho(\eta)$ from (2*a*). (By assuming a constant relaxation time in the rate law, and expanding in small powers of E_v/h, Murzinov actually obtained a closed form expression for $\rho(\eta)$.) The mapping from η to y was obtained by numerically inverting (17). Solutions were presented for a sphere, with the values for R_s and u_{xb} taken from exact numerical solutions for *equilibrium* flow. The results are similar to those of Freeman, except that gradients near the stagnation point are now more accurate.

A still greater refinement of Freeman's method is the mapping technique of Gibson & Marrone (1962*a*). Their independent variable χ, defined by

$$\chi = C\int_0^t p\, dt, \tag{18}$$

is equivalent to Freeman's Θ on the axial streamline, since they also invoked the Newtonian approximation of constant p and h. Noting that for strong shocks the pressure changes in the relaxation zone behind a normal shock wave are also negligible, they obtained $\rho(t)$ from a normal-shock solution rather than the isobaric solution of Freeman. The right-hand side of (13*b*) was approximated by letting $p_{xx} = (p_{xx})_s$, the latter being determined by the shock radius R_s and the known frozen shock conditions. Using (14), equation (13*b*) was then treated as a first-order differential equation for $u_x(t)$, and solved numerically. A simple quadrature then yielded $\rho v(t)$ from (13*a*) and (14). Numerical results using this method may be found in Gibson & Marrone (1962*b*, *c*) for the flow of air behind a catenary shock wave. By varying R_s, conditions ranging from near equilibrium with a thin

reaction zone near the shock wave, to near frozen, where the reaction zone adjoins the body, are shown. In particular, the transition from zero to infinite gradients at the body, to be discussed in §4, is clearly illustrated. In spite of its great accuracy, the method still yields the same stagnation-point state for all conditions, since it maps the identical solution onto the axial streamline.

Turning now to the approaches which do not employ (13*b*), we find the earliest to be the extension to non-equilibrium flow of the method used by Ustinov (1960) to treat the equilibrium blunt-body problem. Ustinov assumed a three-term Taylor series about $y = \delta$ for the function $v(y)$, i.e.

$$v(y) = v(\delta) + \frac{dv}{dy}(\delta)(y-\delta) + \frac{1}{2}\frac{d^2v}{dy^2}(\delta)(y-\delta)^2, \tag{19}$$

where the three coefficients are known functions of a given shock shape and free-stream conditions. Anisimov & Khodyko (1964) evaluated the coefficients for a spherical shock wave with vibrational relaxation. They only carried the method as far as determining the stand-off distance from the condition $v(0) = 0$, indicating how the remainder of the system of equations could be integrated. This was actually carried out by Lun'kin & Shtengel (1964) for a spherical shock wave in a dissociating diatomic gas, although they assumed constant pressure and enthalpy to simplify the calculations. Thus, they integrated equation (12), with the aid of (19), and determined the other variables from (2). Their results differ from those of the other methods in that the density exhibits an overshoot for near-equilibrium flow. This may be due to the poor convergence of the Taylor expansion in this limit, which makes the three-term truncation in (19) a poor approximation. A point of confusion in all three papers is that the solutions are claimed to be for a spherical body, and the needless (and incorrect) assumption is made that the shock wave and body are concentric.

The semi-analytic approach is also a necessary adjunct of scheme I of the numerical method of integration relations (see Belotserkovskii 1966, Hayes & Probstein 1966) in which the shock layer is divided into longitudinal strips. Here the stagnation-point state is needed as an initial condition for the integration along the body. The method was used in the one-strip approximation by Shih & Baron (1964) to treat a sphere in a five-component reacting air mixture, and by Hermann (1965), who considered a circular cylinder in a mixture of reacting O_2 and inert N_2. Both assumed a linear variation of ρu_x with y, which can be written, after manipulation with (13*a*), as

$$\rho u_x = \frac{-2\rho_s v_s}{(1+j)\delta}\left(1-\frac{y}{\delta}\right) - \rho_s u_{xs}\left(1-2\frac{y}{\delta}\right). \tag{20}$$

But the integration of equation (13*c*), combined with (13*a*), and the assumption of a linear variation of $\rho v u_x$ with y, yields the relation

$$p_s - p_b = -\rho_s v_s^2 - \tfrac{1}{2}(1+j)\delta\rho_s v_s u_{xs}. \tag{21}$$

The elimination of $\rho_s u_{xs}$ from (20) and (21) results finally in

$$(1+j)\tfrac{1}{2}\delta v_s \rho u_x = (p_s - p_b)[1-2(y/\delta)] - (y/\delta)\rho_s v_s^2. \tag{22}$$

Equation (22) provides the closing relation to integrate the coupled set of equations numerically for an assumed δ. Unfortunately, the presence of the unknown p_b requires this to be done iteratively. Of the results presented in these two papers, the most significant is figure 5 of Shih & Baron (1964), which shows a spread in stagnation pressures, with the non-equilibrium values lying between the equilibrium and frozen values. (There is no noticeable spread between the equilibrium and non-equilibrium values of temperature and species concentrations.) We note from (22) and (13*a*) that ρv varies quadratically with y, as opposed to the quadratic variation of v with y assumed in (19). Lun'kin & Popov (1964, 1966) used the two-strip approximation to treat a sphere in oxygen. Since both δ and $v(\frac{1}{2}\delta)$ are assumed, they simply utilized a quadratic variation of v with y for their closing relation. Their results, as tabulated in Belotserkovskii (1966), also showed a spread in stagnation pressures.

In comparing the two types of semi-analytic methods, we note that in the mapping techniques a full set of equations was solved approximately, while in the methods not employing (13*b*) a partial, approximate set of equations was integrated exactly. Solutions using the former methods are inherently incapable of resolving differences in stagnation-point states, while results from the latter methods are of questionable accuracy due to the non-analytic nature of the approximating functions (see §4). The final step of combining the advantages of both methods was taken by Conti (1964, 1966), who employed an improved version of the method of series truncations, originally developed by Swigart (1963). Conti treated the flow of a mixture of reacting O_2 and inert N_2 behind a circular cylindrical shock wave (1964) and a spherical shock wave (1966), assuming a cosinusoidal-square variation of the pressure with the polar angle. His first-truncation system of equations is essentially equivalent to equations (2*a*), (12), and (13), with p_{xx} approximated as

$$p_{xx} = (p_{xx})_s p/p_s. \tag{23}$$

The complete system of equations was integrated numerically, using several transformations to facilitate the integration near the stagnation point. In addition to the spread in stagnation-point pressures, Conti also obtained differences in the degree of dissociation and temperature in the fourth and fifth significant figures, respectively. Recently (Conti & Van Dyke 1969*a*), very precise calculations were performed for a Lighthill gas, using a choice of independent variable that was aided by a knowledge of the local behaviour of the solution near the stagnation point. The results clearly show a small (but definite) variation of stagnation-point values of all variables with the degree of non-equilibrium.

Numerical solutions

The earliest numerical treatment is due to Lick (1960), who used the inverse marching technique (see Hayes & Probstein 1966) to solve for the flow of reacting O_2 and inert N_2 behind a catenary shock wave. Unfortunately, the range of shock radii used did not encompass the near-frozen régime covered by other investigators. Although variations in stagnation-point values were found for the

pressure and the degree of dissociation, the latter is incorrect, being actually in the wrong direction (see §5).

Scheme II of the method of integral relations, in which the shock layer is divided into strips normal to the body, was employed in the second approximation by Belotserkovskii & Dushin (1964) to treat a sphere in dissociating O_2 and by Dushin & Lun'kin (1966), who considered a sphere in a five-component reacting air mixture. A compendium of graphical and tabular results from these two papers, as well as other calculations, may be found in Belotserkovskii (1966). The results for the stagnation-point state show large variations in the temperature and species concentrations in the near-frozen régime, in contrast to the very small variations found by Conti (1966). The former are clearly in error (see §5).

Telenin's method (Gilinskiy, Telenin & Tinyakov 1964) was used to investigate the effect of reacting air (Stulov & Telenin 1965), and vibrational relaxation (Stulov & Turchak 1966; Saiapin 1966) in the flow about a sphere. In the near-frozen case, the stagnation-point states were also in error, since they were derived from crude extrapolations. In the paper of Stulov & Turchak, a local analysis (to be described in the next section) was carried out, indicating the presence of infinite gradients. Yet no attempt was made to use this local solution to improve the stagnation-point solution.

The conclusion drawn from the analysis of the numerical solutions is that the relatively coarse grid in physical space necessary to obtain the global solution in the complete shock layer can lead to large errors in the stagnation-point state in the near-frozen limit. This is a direct result of the non-analytic nature of the flow near the stagnation point, which we will now investigate by means of a local solution.

4. Local stagnation-point analysis

In this section we generalize the results of Conti & Van Dyke (1969*a*) for the local solution near the stagnation point, to arbitrary non-equilibrium processes, following the (suitably corrected) arguments of Stulov & Turchak (1966). Using the differential form of (2*a*):

$$\frac{d\rho}{dy} = \left(\frac{\partial\rho}{\partial p}\right)_{h,q_i}\frac{dp}{dy} + \left(\frac{\partial\rho}{\partial h}\right)_{p,q_i}\frac{dh}{dy} + \sum_{i=1}^{n}\left(\frac{\partial\rho}{\partial q_i}\right)_{p,h,q_j}\frac{dq_i}{dy} \tag{24}$$

(where the subscript q_j indicates that all other q_j ($j \neq i$) are held constant in the differentiation), equation (13*a*) can be combined with (13*c*), (13*d*), (12) and (13*b*) to yield

$$-(1+j)\rho u_x = \rho\frac{dy}{dv}\left(1-\frac{v^2}{a_f^2}\right) + \sum_{i=1}^{n}\sum_{r=1}^{m}\left(\frac{\partial\rho}{\partial q_i}\right)_{p,h,q_j}\omega_{i,r}. \tag{25}$$

For smooth nose shapes, p_{xx} must be finite at the stagnation point. From (13*b*) it follows that u_{xb} is finite. Since all $\omega_{i,r}$ are assumed finite, it follows from (25) that dv/dy is finite at the stagnation point. Let us define

$$(dv/dy)_b \equiv -C, \tag{26}$$

where the finite constant $C > 0$ must be determined from a global solution. Consider a point on the axis where $v = v_1$, and $|v_1/v_s| \ll 1$. If $\rho_{\max}$ is the maximum value of ρ between this point and the stagnation point, it follows from (13*c*) and (13*d*) that

$$p_b - p_1 \leqslant \rho_{\max} \tfrac{1}{2} v_1^2. \tag{27}$$

Furthermore, since $v \simeq Cy$ near the stagnation point, one sees from (14) that a fluid particle requires a logarithmically infinite time to reach the body from point 1. But (13*d*) and (27) show that pressure and enthalpy changes are negligible during this process. The fluid particle therefore essentially undergoes an isobaric process in time and must reach a state of complete thermodynamic equilibrium at the body. Thus, the thermodynamic state at the body is an equilibrium state, and is a unique function of p_b and h_b. Whereas for given free-stream conditions it follows from (13*d*) that

$$h_b = h_\infty + \tfrac{1}{2} U_\infty^2, \tag{28}$$

the pressure p_b cannot be determine from the local analysis. We will show in §5 that bounds on p_b can be simply established. The actual determination of p_b from a simplified global analysis will be discussed in §6. Since $(\omega_{i,r})_b = 0$, equations (25) and (26) lead immediately to

$$u_{xb} = C/(1+j). \tag{29}$$

The local analysis can also determine the manner in which the state variables approach their stagnation-point values. From equations (13*c*), (13*d*), (26) and (28) we can write

$$p \approx p_b - \rho_b \tfrac{1}{2} C^2 y^2 \tag{30a}$$

and

$$h \approx h_b - \tfrac{1}{2} C^2 y^2 \tag{30b}$$

for small y. Defining q_i' by

$$q_i = q_{ib} + q_i' = q_i^*(p_b, h_b) + q_i', \tag{31}$$

and noting that $(\chi_{i,r})_b = 0$, it follows from (30) and (31) that

$$\chi_{i,r} \approx -\left[\rho \left(\frac{\partial \chi_{i,r}}{\partial p}\right)_{h,q_j} + \left(\frac{\partial \chi_{i,r}}{\partial h}\right)_{p,q_j}\right]_b \tfrac{1}{2} C^2 y^2 + \sum_{j=1}^{n} \left[\left(\frac{\partial \chi_{i,r}}{\partial q_j}\right)_{p,h,q_k}\right]_b q_j'. \tag{32}$$

With the aid of (5) and (32), equation (12) can then be written in the form

$$y \frac{dq_i'}{dy} \approx \sum_{j=1}^{n} B_{ij} q_j' + A_i y^2, \tag{33}$$

where

$$A_i \equiv \tfrac{1}{2} C \sum_{r=1}^{m} \left\{\frac{1}{\tau_{i,r}} \left[\rho \left(\frac{\partial \chi_{i,r}}{\partial p}\right)_{h,q_j} + \left(\frac{\partial \chi_{i\,r}}{\partial h}\right)_{p,q_j}\right]\right\}_b \tag{34}$$

and

$$B_{ij} \equiv -\frac{1}{C} \sum_{r=1}^{m} \left[\frac{1}{\tau_{i,r}} \left(\frac{\partial \chi_{i,r}}{\partial q_j}\right)_{p,h,q_k}\right]_b. \tag{35}$$

The general solution of (33) takes the form

$$q_i' = \sum_{k=1}^{n} a_k C_i^k y^{\lambda_k} + K_i y^2, \tag{36}$$

where λ_k is the kth eigenvalue of B_{ij}, C_i^k is the ith component of the eigenvector belonging to λ_k, and K_i is obtained from the solution of the matrix equation

$$\sum_{j=1}^{\infty} (B_{ij} - 2\delta_{ij})\, K_j = -A_i. \tag{37}$$

Since q_i' is real, and $q_i'(0) = 0$, it follows that λ_k is real and positive for all k. (This has been rigorously proved for chemical non-equilibrium by Emanuel 1963.) The constants a_k must be determined from a global solution.

The dominant behaviour of q_i' near the stagnation point depends on whether the minimum value of λ_k is greater or less than 2. In making the comparison, we must exclude those values of k for which the global solution gives $a_k = 0$. Furthermore, a particular non-equilibrium variable q_i may have a zero value of the eigenvector component C_i^k for some k. We therefore define

$$\lambda_i \equiv \text{minimum value of } \lambda_k \text{ for which } C_i \equiv a_k C_i^k \neq 0.$$

Noting that solution (36) must be modified if λ_k is degenerate or equal to 2, we can state the following general results for the dominant behaviour of q_i near the stagnation point:

(*a*) If $\lambda_i > 2$,

$$q_i \approx q_{ib} + K_i y^2. \tag{38}$$

(*b*) If $\lambda_i = 2$, and is of multiplicity p,

$$q_i \approx q_{ib} + C_i y^2 (\log y)^m, \tag{39}$$

where m is a positive integer satisfying $1 \leqslant m \leqslant p$.

(*c*) If $\lambda_i < 2$, and is of multiplicity p,

$$q_i \approx q_{ib} + C_i y^{\lambda_i} (\log y)^m, \tag{40}$$

where m is a positive integer satisfying $0 \leqslant m \leqslant p-1$.

One can therefore conclude that if $\lambda_i > 2$, the variable q_i has the same algebraic behaviour exhibited by the pressure and enthalpy, and it approaches its stagnation-point value with a zero slope. If $\lambda_i > 2$ for all i, then this statement holds for all thermodynamic state variables. If on the other hand, $\lambda_i \leqslant 2$, q_i has a non-analytic behaviour near the stagnation point. The stagnation-point gradient is still zero as long at $\lambda_i > 1$. The gradient becomes infinite when $\lambda_i \leqslant 1$ (except for the case $\lambda_i = 1$, $m = 0$, when the gradient is finite.) Since λ_i may have different values for the various non-equilibrium variables q_i, we see that some q_i may approach the stagnation point with a zero slope, while others with an infinite slope. The behaviour of the other thermodynamic variables is determined by the minimum value of λ_i possessed by those variables q_i on which they are functionally dependent, as given by (2).

For a single non-equilibrium variable, our results are in agreement with those of Conti & Van Dyke (1969*a*), who performed a more formal local analysis for the dissociation of a Lighthill gas. The analysis of Stulov & Turchak (1966) for vibrational relaxation, whose basic line of argument was followed here, contains two flaws. Their proof of the attainment of equilibrium at the stagnation point was restricted by the assumption of a linear relaxation model for the rate law.

They also neglected pressure and enthalpy changes near the stagnation point. Thus, the term corresponding to our $K_i y^2$ in equation (36) was missing in their solution. Consequently, the algebraic behaviour of solution (38), which one must always obtain for a flow that is sufficiently close to an equilbrium flow, was absent from their results.

The results of this section clearly show that great care must be exercised in integrating the coupled equations near the stagnation point. The discrepancy in reported stagnation-point values of state variables (other than p or h) from numerical solutions is easily understood. Although the local analysis proves that the stagnation-point state is an equilibrium state, it cannot determine what this state is. Since the state can be approached in a non-analytic manner, and is the result of a global solution, dependent on body shape and rate laws, it would seem at first glance to be difficult to determine. Fortunately, equation (30a) shows that the pressure behaves algebraically near the stagnation point. This will enable us to determine simply bounds on the range of its possible values, as shown in the next section.

5. Equilibrium and frozen limits

Classification of limiting stagnation-point states

It was stated in § 2 that the relaxation times $\tau_{i,r}$ are always finite and non-zero in magnitude under real conditions. Thus, the concept of equilibrium (or frozen) *flow* can only be regarded as being derived from the mathematical limit $\tau_{i,r} \to 0$ (or ∞) for all $\tau_{i,r}$. The stagnation-point state is similarly obtained from the limit $y \to 0$, or equivalently, $t \to \infty$, where t is the Lagrangian particle time. Since equilibrium (or frozen) stagnation-point states are therefore defined in terms of double limits, one must specify the order in which the limits are taken. This leads to two types of limiting stagnation-point states. The first is obtained by taking the limit of equilibrium (or frozen) flow, i.e. $\tau_{i,r} \to 0$ (or ∞), and then letting the flow reach the stagnation point ($y \to 0$). We shall refer to such a state simply as an *equilibrium* (or *frozen*) state. The other state is defined by letting a non-equilibrium flow reach the stagnation point ($y \to 0$), and then considering the limit of such a state as $\tau_{i,r} \to 0$ (or ∞). We will refer to this second type of state by the term *equilibrium* (or *frozen*) *limit*. It is clear that the latter type of limiting state must be used in determining bounds on the set of possible stagnation-point states in non-equilibrium flow.

The four limiting stagnation-point states defined above are simply calculable from the state equations and free-stream conditions, as is shown below:

(i) *Equilibrium.* Since $\tau_{i,r} = 0$ for all i, r, the state immediately behind the shock is an equilibrium state, and its calculation was discussed in § 2. Denoting this state by the subscript se we can calculate the specific entropy from

$$S_{se} = S^*(p_{se}, h_{se}). \tag{41}$$

An equilibrium, adiabatic flow is isentropic. The equilibrium stagnation-point state, denoted by be, is thus determined by the condition

$$S_{be} = S_{se}. \tag{42}$$

From equation (1*d*) it follows that the stagnation-point enthalpy is always given by

$$h_b = h_t \equiv h_\infty + \tfrac{1}{2}U_\infty^2. \tag{43}$$

Therefore, the stagnation-point pressure is given by the iterative solution of

$$S_{se} = S^*(p_{be}, h_t), \tag{44}$$

and the remaining state variables are then determined from (7) and (8).

(ii) *Frozen.* The frozen conditions behind the shock, denoted by *sf*, were also discussed in §2. The specific entropy is determined from (2*b*) as

$$S_{sf} = S(p_{sf}, h_{sf}, q_{1\infty}, q_{2\infty}, \ldots, q_{n\infty}). \tag{45}$$

A frozen flow is also isentropic, and the non-equilibrium variables remain frozen at their values behind the shock. The frozen stagnation-point state, denoted by *bf*, is thus determined by iteratively solving for the pressure from

$$S_{sf} = S(p_{bf}, h_t, q_{1\infty}, q_{2\infty}, \ldots, q_{n\infty}). \tag{46}$$

(iii) *Equilibrium limit.* We will denote the stagnation-point conditions in the equilibrium limit by the subscript *bel*. It is easy to demonstrate that this state is identical to the equilibrium state (case (i)), i.e.

$$\phi_{bel} = \phi_{be}, \tag{47}$$

where ϕ stands for any state variable. Consider a very small Lagrange time t_2 after a fluid particle has crossed the shock wave. From equations (10*a*), (13*a*) and (14) it follows that

$$|\rho_2 v_2 - \rho_s v_s| \leqslant (1+j)\rho_\infty U_\infty (u_x)_{\max} t_2, \tag{48}$$

where $(u_x)_{\max}$ is the maximum value of u_x between the shock and point 2. By taking t_2 sufficiently small, the flow up to that time will deviate very little from the one-dimensional flow behind a normal shock wave. If all $\tau_{i,r} \ll t_2$, the fluid particle at time t_2 will have essentially undergone a one-dimensional relaxation, and approached the equilibrium shock conditions as closely as desired. For all times $t > t_2$, the particle will remain as close to equilibrium as desired, if all $\tau_{i,r}$ remain sufficiently small. In the limit $\tau_{i,r} \to 0$, we obtain a discontinuous jump from conditions *sf* to *se* at the shock wave, and conditions at the body are given by (47).

(iv) *Frozen limit.* The stagnation-point state in the frozen limit, denoted by *bfl*, is not expected to be the same as the frozen state (case (ii)), since the former is an equilibrium state (as proved in §4), while the latter is out of equilibrium. One can readily show though that

$$p_{bfl} = p_{bf}. \tag{49}$$

Consider again the point on the axis close to the body where $|v_1/v_s| \ll 1$ (see §4). Since the particle-flow time from the shock wave to this point is finite, one can approach frozen conditions corresponding to this velocity as closely as possible by letting all $\tau_{i,r}$ be sufficiently large. Specifically, for a fixed v_1, one can obtain $|(p_1 - p_{1f})/\rho_\infty U_\infty^2| = O[(v_1/v_s)^2]$, where p_{1f} is the frozen pressure corresponding

to v_1. Equation (27) shows that both in the non-equilibrium and frozen flows, additional fractional pressure changes between this point and the stagnation point are also of $O[(v_1/v_s)^2]$. We thus arrive at

$$|(p_b - p_{bf})/\rho_\infty U_\infty^2| = O[(v_1/v_s)^2]. \tag{50}$$

In the limit $\tau_{i,r} \to \infty$, the non-equilibrium flow therefore first reaches the frozen conditions at the stagnation point, and then undergoes an adiabatic relaxation process at rest, in which the pressure and enthalpy remain fixed, but the other state variables assume equilibrium values. Thus, for example, the entropy in the frozen limit is given by

$$S_{bfl} = S^*(p_{bf}, h_t), \tag{51}$$

while the frozen entropy $S_{bf} = S_{sf}$ is given by (45). The uniform behaviour of the pressure, and the non-uniform behaviour of the other variables could have been anticipated from the results of the local analysis of §4.

We will demonstrate in §6 that p_{be} and p_{bf} do in fact give bounds on possible stagnation-point pressures. We show next that to a very high approximation, the range of variation of this pressure depends solely on the equilibrium and frozen shock density-ratios.

Relation of stagnation-point pressures to shock density ratio

The stagnation-point pressures for the two limiting cases of equilibrium and frozen flow are determined in an analogous manner from the shock conditions, since both result from an isentropic compression. Consequently, all the subsequent relations in which the variables are not otherwise identified, are assumed to be valid for either equilibrium or frozen flow.

The shock conditions will be expressed in terms of the shock density-ratio

$$\epsilon \equiv \rho_\infty/\rho_s = -v_s/U_\infty. \tag{52}$$

The compression along the axis of symmetry is governed by the local isentropic exponent γ, defined by

$$\gamma = \left(\frac{\partial \log p}{\partial \log \rho}\right)_S = \rho a^2/p, \tag{53}$$

where a is the local speed of sound. Although γ is not constant, its variation from the shock to the body is small. A fairly general bound is given by

$$|\gamma_b - \gamma_s| \leqslant O(\epsilon^2). \tag{54}$$

Since the fractional change in enthalpy is of $O(\epsilon^2)$, as shown by (13*d*), equation (43) follows from the relation $|h(\partial\gamma/\partial h)_S| \leqslant O(1)$, which should be satisfied under most conditions. It is valid for equilibrium air, as shown in figure 4 of Moeckel & Weston (1958).

Within the accuracy that γ is constant, it can be expressed as a function of ϵ alone. The precise conditions for this statement to hold require first the determination of ϵ. The equation of state on either side of the shock wave can be written in the form

$$h = \frac{\gamma}{\gamma - 1}\frac{p}{\rho} + A, \tag{55}$$

which can be considered the defining equation for A. In order to include the case of a non-equilibrium free stream, we take for the isentropic exponent γ_∞ the frozen value $\gamma_{\infty f}$. A_∞ would then represent the energy of the internal modes that are out of equilibrium with the translational mode. The values of γ_{se} and A_{se} behind a shock wave for the equilibrium flow of air have been plotted for various flight and shock-tube conditions by Sanders (1958).

With γ and A assumed specified, equations (10) and (55) can be combined to yield the following solution for ϵ:

$$\epsilon = \frac{\gamma_s}{(\gamma_s+1)}\left[1+\frac{1}{\gamma_\infty M_\infty^2}\right] - \frac{1}{(\gamma_s+1)}\left[1-2(\bar{A}_\infty-\bar{A}_s)(\gamma_s^2-1)+\frac{2(\gamma_\infty-\gamma_s^2)}{\gamma_\infty(\gamma_\infty-1)M_\infty^2}+\frac{\gamma_s^2}{\gamma_\infty^2 M_\infty^4}\right]^{\frac{1}{2}}, \tag{56}$$

where we have introduced the free-stream frozen Mach number $M_\infty = U_\infty/a_{\infty f}$, and the non-dimensionalization $\bar{A} = A/U_\infty^2$. If we now assume that

$$\frac{1}{(\gamma_\infty-1)M_\infty^2} = O(\epsilon) \quad \text{and} \quad |\bar{A}_\infty-\bar{A}_s| = O(\epsilon), \tag{57}$$

it follows from (54), (56) and (57) that

$$1/\gamma = 1-2\epsilon+O(\epsilon^2) \tag{58}$$

between the shock and the body. The graphical data of Sanders (1958) show that the second relation (57) is satisfied for equilibrium air flows under most conditions.

Introducing the non-dimensional variables

$$\bar{p} = \frac{p}{\rho_\infty U_\infty^2}, \quad \bar{\rho} = \frac{\rho}{\rho_\infty}, \quad \text{and} \quad \bar{v} = \frac{v}{U_\infty},$$

we obtain from (10a), (10b), (52) and (53) for the pressure behind the shock wave

$$\bar{p}_s = 1-\epsilon+\frac{1}{\gamma_\infty M_\infty^2}, \tag{59}$$

while (13c) and (53) (with γ constant) result in

$$\epsilon\bar{\rho}(\bar{v}) = \left[1+\frac{1}{\bar{p}_s}\int_{\bar{v}}^{-\epsilon}\bar{\rho}(\bar{v})\,\bar{v}\,d\bar{v}\right]^{1/\gamma}. \tag{60}$$

Equation (60) can be solved iteratively for $\bar{\rho}(\bar{v})$ starting with the first approximation $\bar{\rho}^{(0)} = 1/\epsilon$. If we use (58) and (59), with the further assumption that

$$\frac{1}{\gamma_\infty M_\infty^2} = O(\epsilon^2), \tag{61}$$

one can carry the iteration of $\bar{\rho}(\bar{v})$ through the third approximation. Combining the result with (13c), we obtain finally

$$\bar{p}_b-\bar{p}_s = \tfrac{1}{2}\epsilon+\tfrac{1}{8}\epsilon^2-\tfrac{5}{48}\epsilon^3+O(\epsilon^4). \tag{62}$$

The stagnation pressure in either equilibrium or frozen flow is thus obtained from (59) and (62). The maximum range of variation of non-dimensional stagnation pressures in a non-equilibrium flow is therefore

$$\bar{p}_{be}-\bar{p}_{bf} = \tfrac{1}{2}(\epsilon_f-\epsilon_e)\,[1-\tfrac{1}{4}(\epsilon_f+\epsilon_e)+\tfrac{5}{24}(\epsilon_f^2+\epsilon_f\epsilon_e+\epsilon_e^2)]+O(\epsilon^4). \tag{63}$$

Since (62) is quite accurate even for density ratios as high as $\epsilon \sim \frac{1}{2}$, we note from (57) and (61) that the approximation can be used for shock waves as weak as $M_\infty \sim 2$. Thus, relations (62) and (63) should be useful for most non-equilibrium flow situations, including those found in the laboratory.

Bounds on stagnation-point state variables

Equation (63) shows that the signs of $p_{be}-p_{bf}$ and $\epsilon_f-\epsilon_e$ are the same. Thus, it is natural to distinguish between two classes of non-equilibrium blunt-body flows. We will denote as *ordinary* flows those for which $\epsilon_f > \epsilon_e$, since this is the situation normally encountered with cold, equilibrium free streams. Non-equilibrium free streams, such as an overdissociated nozzle flow, can result in $\epsilon_e > \epsilon_f$, which we associate with an *extraordinary* flow. It follows from (63) that

$$p_{be} \gtrless p_{bf} \quad \text{for} \quad \left\{\begin{matrix}\text{ordinary}\\ \text{extraordinary}\end{matrix}\right\} \text{flows}\dagger. \tag{64}$$

A quantitative estimate of the spread in stagnation-point pressures may be obtained by considering a strong shock wave in cold air for which $\epsilon_f = \frac{1}{6}$, and ϵ_e may be as low as $\frac{1}{15}$. The maximum fractional spread in pressure is approximately $(\Delta p/p)_b = 0{\cdot}05$.

The direction and magnitude of the spread in any other stagnation-point state variable ϕ is obtained in terms of the spread in pressure from the thermodynamic derivative $(\partial\phi^*/\partial p)_h$, since the states are all equilibrium states at the same total enthalpy. A general statement can be made about the entropy, since the first and second laws of thermodynamics yield the relation

$$(\partial S^*/\partial p)_h = -1/\rho T < 0. \tag{65}$$

It follows from (64) and (65) that

$$S_{bfl} \gtrless S_{be} \quad \text{for} \quad \left\{\begin{matrix}\text{ordinary}\\ \text{extraordinary}\end{matrix}\right\} \text{flows}. \tag{66}$$

Since the relaxation process behind a normal shock wave is irreversible, $S_{se} > S_{sf}$ for either type of flow. It follows that

$$S_{be} > S_{bf}. \tag{67}$$

For ordinary flows, we see from (66) and (67) that the change in entropy due to the relaxation at rest from the frozen state at the stagnation point is greater than the entropy change due to the one-dimensional relaxation from the frozen state behind the shock wave. Thus, the stagnation-point entropy is not bounded by

† This statement is only valid within a relative error of $O(\epsilon^4)$. If $\epsilon_f = \epsilon_e$, one can show that $p_{be}-p_{bf} = \frac{1}{2}(A_{sf}-A_{se})\epsilon^3 > 0$. (The sign follows from the general relation $a_f > a_e$.) Therefore, there exists a narrow range of extraordinary flows for which $p_{be} > p_{bf}$.

the frozen and equilibrium values, but actually exhibits an *overshoot* of the equilibrium entropy. This overshoot will not occur for extraordinary flows.

If the non-equilibrium processes involve only internal modes of species (rotational or vibrational relaxation, electronic excitation), then the equilibrium temperature $T = T^*(h)$ only. Therefore, $T_b = T^*(h_t)$, a unique value for all stagnation-point states. Since $q_{ib} = q_i^*(T_b)$ for all internal non-equilibrium variables, they also have unique values. The density at the body is proportional to the pressure under these conditions, and its variation is thus determined by the variation of the pressure. It is easy to show that the density does not exhibit an overshoot or undershoot for either type of flow.

If the non-equilibrium processes involve the creation or destruction of species (dissociation, ionization), then $T_b = T^*(p_b, h_t)$. The laws of thermodynamics impose no restriction on the sign of $(\partial T^*/\partial p)_h$. For the dissociation and ionization of air, both signs are possible, but the negative sign is found only in regions of very high density where virial effects are important and non-equilibrium phenomena are essentially absent. We thus obtain the condition

$$T_{be} \gtrless T_{bfl} \quad \text{for} \quad \left\{\begin{matrix}\text{ordinary} \\ \text{extraordinary}\end{matrix}\right\} \text{flows.} \tag{68}$$

It is easy to demonstrate that the stagnation-point temperature exhibits an undershoot (overshoot) of the equilibrium temperature for ordinary (extraordinary) flows. Since the sign of $(\partial q_i^*/\partial p)_h$ depends on the individual non-equilibrium variable q_i, no general statement can be made concerning its behaviour. If q_i represents an internal mode of a species (as in coupled vibrational and chemical non-equilibrium) its variation at the stagnation point is determined from the variation of the temperature (68), since $dq_i^*/dT > 0$. There is no overshoot or undershoot for such a variable. The total number of particles per unit mass is proportional to the compressibility factor Z appearing in the thermal equation of state $p = \rho Z R_0 T$ where R_0 is the undissociated, low temperature gas constant. (For the dissociation of a single diatomic gas, $Z = 1 + \alpha$, where α is the atom mass fraction.) Since $(\partial Z^*/\partial p)_h < 0$, (see Moeckel & Weston 1958), we have

$$Z_{bfl} \gtrless Z_{be} \quad \text{for} \quad \left\{\begin{matrix}\text{ordinary} \\ \text{extraordinary}\end{matrix}\right\} \text{flows,} \tag{69}$$

and the stagnation-point compressibility factor exhibits an overshoot (undershoot) of the equilibrium value for ordinary (extraordinary) flows. The data of Moeckel & Weston shows that

$$|(\partial \log T^*/\partial \log p)_h| \ll 1 \quad \text{and} \quad |(\partial \log Z^*/\partial \log p)_h| \gg 1.$$

Thus, the density has the same behaviour as in the case involving internal modes only.

Critique of published results

For a typical non-equilibrium situation we consider the flow of air at a speed of 14 000 ft./sec and an altitude of 100 000 ft. This was the case essentially considered by Lick (1960) and Conti (1966). If we let $\Delta\phi \equiv \phi_{be} - \phi_{bfl}$ be the maximum spread

in the stagnation-point values of the variable ϕ, we find from exact calculations that

$$\Delta p/p = 0{\cdot}0385, \quad \Delta S/(S_e - S_f) = -0{\cdot}0178, \quad \Delta T = 5{\cdot}4\,^\circ\mathrm{K}, \quad \Delta Z = -0{\cdot}0004, \tag{70}$$

where $T_b = 4820\,^\circ\mathrm{K}$ and $Z_b = 1{\cdot}18$. Conti's (unpublished) numerical data are consistent with these results. On the other hand, the relative values of the mass fraction of atomic oxygen α_O as shown in figure 10 of Lick's (1960) paper are obviously in error at the stagnation point. From equation (69), it follows that the value for his $\chi = 100$ ('practically' equilibrium) should be *lower* than that for $\chi = 5$ ('partial' equilibrium), while the reverse is shown in the figure. Based on the difference in pressure, the difference in the values of α_O should be approximately 6×10^{-5}, instead of the much larger value of 4×10^{-3} that is indicated. This error in both sign and magnitude suggests that the $\chi = 5$ curve for the axial variation of α_O must possess an infinite gradient at the stagnation point ($\lambda_O < 1$), although its global behaviour (see figure 5 of Lick's paper) implies otherwise. (This type of phenomenon has been clearly demonstrated by Conti & Van Dyke (1969*a*), see their figure 4, $K = 0{\cdot}9975$).

$M_\infty = 10$, $p_\infty = 0{\cdot}001$ atm, $T_\infty = 290\,^\circ\mathrm{K}$

$R_b(m)$	$\dfrac{p_b}{2\rho_\infty h_t}$	$\dfrac{T_b R_0}{2h_t}$	$\dfrac{\rho_b}{\rho_\infty}$	α_{O_b}	Table no. in ref.
1000	0·916	0·0704	11·462	0·134	3·17
0·01	0·900	0·0885	9·461	0·0743	3·9

TABLE 1. Stagnation-point variables for the non-equilibrium flow of oxygen past a sphere, as calculated by scheme II of the method of integral relations (from Belotserkovskii 1966)

The dangers inherent in continuing a numerical integration near the stagnation point by simple extrapolations are particularly great for the near frozen régime. This is given a striking illustration by considering the results of numerical solutions employing scheme II of the method of integral relations, as tabulated in Belotserkovskii (1966). As an example, table 1 presents results for several dimensionless stagnation-point variables for the flow of dissociating oxygen past a sphere. Two cases, one for a body radius $R_b = 1000$ m (near equilibrium) and the other for $R_b = 0{\cdot}01$ m (near frozen), are shown. From the results of (70), it follows (within three significant figures) that there should be no difference in T or α_O between the two cases. Yet table 1 clearly shows a significant difference (*in the wrong direction*), which is almost a *factor of two* for the atomic mass fraction of oxygen. The density is also seriously in error, since it should be proportional to the pressure, and show less than a 2 % difference.

The above examples show that although the stagnation-point state is always found in a narrow range on one side of the state determined by equilibrium flow, we must exercise great care in its calculation via numerical integration from the shock wave. This has been successfully accomplished by Conti & Van Dyke (1969*a*), who employed appropriate change of variables guided by the local

solution. Results for a Lighthill gas, accurate to five significant figures, are shown in their table 1, and are found to be in agreement with our results. It would be useful to be able to predict the stagnation-point state accurately without having to resort to an elaborate numerical integration for each new non-equilibrium flow condition. A simple method of accomplishing this is described in the next section.

6. Prediction of stagnation-point state

In this section we assume that the free-stream conditions and the equation of state for the gas are specified. This determines the equilibrium and frozen limits for the stagnation-point state, as discussed in §5. The actual stagnation-point state is influenced by two independent factors. One is the non-equilibrium processes, which are characterized by the generalized rate equations (4) to (6). The other is the flow geometry determined by the shape and scale of the body. For reasons stated at the end of §4, it is simplest to predict the pressure. Within an error of $O(\epsilon)$, the effect of the two factors on the variation of the pressure can be uncoupled, and the effect of the flow geometry is contained only in its scale (through the shock radius R_s). This will enable us to express the stagnation-point pressure in terms of a simple quadrature.

The pressure change from the shock to the body can be found from (13*c*). After an integration by parts, it can be written (in non-dimensional form) as

$$\bar{p}_b - \bar{p}_{sf} = \epsilon_f + \int_{-1}^{0} \frac{\bar{\rho}\bar{v}}{\bar{\rho}}\, d(\bar{\rho}\bar{v}). \tag{71}$$

The relation between $\bar{\rho}$ and $\bar{\rho}\bar{v}$ is found implicitly by introducing as independent variable the Lagrangian particle time t. Following Gibson & Marrone (1962*a*) we note that both in the blunt-body flow and the relaxation zone behind a normal shock wave, the fractional change in pressure is of $O(\epsilon)$. We thus approximate the density in the denominator of the integrand by

$$\bar{\rho}(t) \approx \bar{\rho}_{ns}(t), \tag{72}$$

where the subscript *ns* indicates the normal-shock solution. Rather than follow the method of Gibson & Marrone (1962*a*) to determine $\bar{\rho}\bar{v}(t)$, it is sufficient within the accuracy of equation (72) to employ Freeman's (1958) approximation of neglecting the pressure term in (13*b*). Introducing the shock radius R_s to define the non-dimensional variables

$$\bar{x} = x/R_s, \quad \bar{t} = tU_\infty/R_s,$$

one can readily show that at the shock wave

$$(\bar{u}_{\bar{x}})_s = 1 - \epsilon_f, \quad \left(\frac{1}{\bar{\rho}}\bar{p}_{\bar{x}\bar{x}}\right)_s = -2\epsilon_f(1-\epsilon_f). \tag{73}$$

Within an error of $O(\epsilon)$, (13*b*), (14) and (73) can be combined to yield

$$\frac{d}{d\bar{t}}(\bar{u}_{\bar{x}}) + \bar{u}_{\bar{x}}^2 \simeq 0; \quad \bar{u}_{\bar{x}}(0) \approx 1, \tag{74}$$

whose solution is

$$\bar{u}_{\bar{x}} \approx (1+\bar{t})^{-1}. \tag{75}$$

As discussed in §3, the approximation leading to (74) breaks down at the stagnation point. This is evident from solution (75), which predicts a zero stagnation-point velocity gradient. However, for the present purposes, this 'outer' solution is perfectly adequate. The neglect of the pressure term in (74) can be shown to lead to large errors in $\bar{\rho}\bar{v}$ only when $|\bar{\rho}\bar{v}|$ is of $O(\epsilon)$, but by then the contribution to the integral in (71) is of $O(\epsilon^3)$, and is therefore negligible within our approximation. Solution (75) must be used with caution; e.g. it leads to an infinite stand-off distance δ for plane flow. The appropriate solution for this latter case is discussed in the appendix.

Equations (13*a*), (14) and (75) are readily combined to yield a first-order equation for $\bar{\rho}\bar{v}(\bar{t})$ whose solution is

$$\bar{\rho}\bar{v} \approx -(1+\bar{t})^{-(1+j)}. \tag{76}$$

Substituting (72) and (76) in equation (71) we obtain for the stagnation-point pressure the relation

$$\bar{p}_b - \bar{p}_{sf} \approx \epsilon_f - (1+j)\frac{U_\infty}{R_s}\int_0^\infty \frac{1}{\bar{\rho}_{ns}(t)}\left(1+\frac{tU_\infty}{R_s}\right)^{-(3+2j)} dt. \tag{77}$$

The integral can be evaluated in the limits of equilibrium (or frozen) flow, for which $\bar{\rho}_{ns} = \epsilon_e^{-1}$ (or ϵ_f^{-1}). One thus obtains

$$\bar{p}_{be} - \bar{p}_{sf} \approx \epsilon_f - \tfrac{1}{2}\epsilon_e, \tag{78a}$$

and

$$\bar{p}_{bf} - \bar{p}_{sf} \approx \tfrac{1}{2}\epsilon_f. \tag{78b}$$

A comparison with (59) and (62) shows that equations (78) are correct to the first order in ϵ, but underestimate the exact values. Eliminating $\bar{p}_{sf}$ from (77) and (78), we obtain the final result

$$\frac{\bar{p}_b - \bar{p}_{bf}}{\bar{p}_{be} - \bar{p}_{bf}} = \frac{\epsilon_f - 2(1+j)\dfrac{U_\infty}{R_s}\displaystyle\int_0^\infty \frac{1}{\bar{\rho}_{ns}(t)}\left(1+\frac{tU_\infty}{R_s}\right)^{-(3+2j)} dt}{\epsilon_f - \epsilon_e} \tag{79a}$$

$$= \frac{-\displaystyle\int_0^\infty \frac{d}{dt}(\bar{\rho}_{ns}^{-1})\left(1+\frac{tU_\infty}{R_s}\right)^{-2(1+j)} dt}{\epsilon_f - \epsilon_e}, \tag{79b}$$

where the second form follows from an integration by parts. If we use the *exact* values for $\bar{p}_{be}$ and $\bar{p}_{bf}$, equations (79) should be highly accurate.†

Equations (79) can be used to study the effects of each of the two factors that influence the stagnation-point pressure. If the rate processes are specified, the normal-shock solution $\bar{\rho}_{ns}(t)$ can be determined. The effect of the scale of the flow can then be studied by evaluating either of the integrals (79) for different values of R_s. We note from (79*b*) that if $\bar{\rho}_{ns}(t)$ varies monotonically with time, $\bar{p}_b$ is a monotonic function of R_s. If, on the other hand, we fix the scale of the flow by specifying R_s, the effect of various rate equations can be investigated by calculating the corresponding solutions for $\bar{\rho}_{ns}(t)$, and evaluating the appropriate integral. If $\bar{\rho}_{ns}(t)$ is always bounded by ϵ_f^{-1} and ϵ_e^{-1} (not necessarily a monotonic

† The expressions are not valid when $\epsilon_f = \epsilon_e$. For this case the uncoupling of the rate processes from the dynamics is invalid.

function of time), it follows from (79a) that the stagnation-point pressure will always lie between its frozen and equilibrium values.

The combined effects of the rate processes and scale of the flow can be studied simply if the density variation is governed by a single parameter. Following Hayes & Probstein (1966), we will assume a single relaxation model for the inverse density of the form

$$\bar{\rho}_{ns}^{-1}(t) = e_e + (e_f - e_e)e^{-t/\tau}, \tag{80}$$

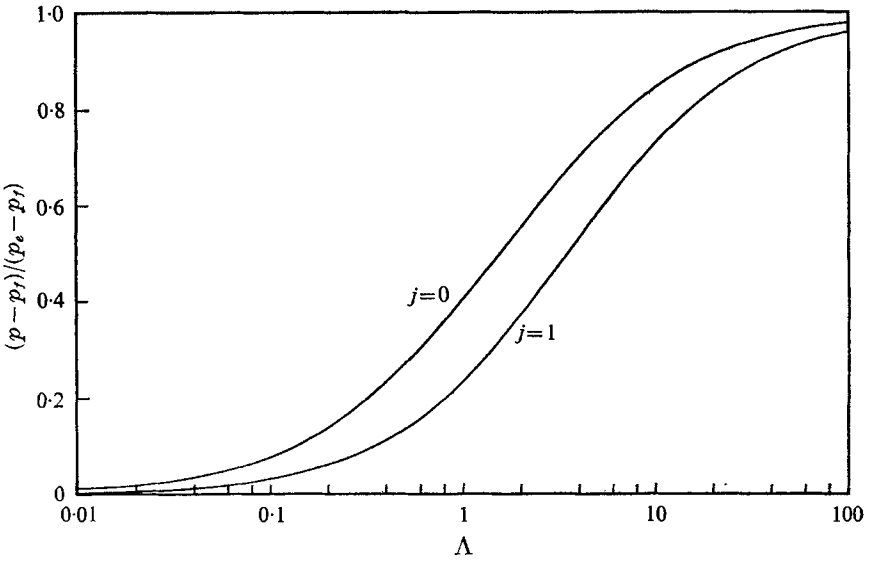

FIGURE 2. Stagnation-point pressure as a function of the reaction parameter Λ for $j = 0$ (plane flow) and $j = 1$ (axisymmetric flow).

where the *constant* relaxation time τ is not to be confused with the local relaxation time $\tau_{i,r}$ for the variable q_i in reaction r appearing in (5). Upon the substitution of (80) into equations (79) we obtain

$$\frac{\bar{p}_b - \bar{p}_{bf}}{\bar{p}_{be} - \bar{p}_{bf}} = 1 - 2(1+j)e^{\Lambda}E_{3+2j}(\Lambda) \tag{81a}$$

$$= \Lambda e^{\Lambda}E_{2(1+j)}(\Lambda), \tag{81b}$$

where the parameter

$$\Lambda = R_s/U_\infty\tau \tag{82}$$

varies between zero (frozen flow) and infinity (equilibrium flow), and

$$E_n(\Lambda) = \int_1^\infty s^{-n}e^{-\Lambda s}ds. \tag{83}$$

The variation of the pressure with Λ according to (81) is shown in figure 2 for plane flow ($j = 0$) and axisymmetric flow ($j = 1$). We note that the pressure is always closer to the equilibrium value for plane than for axisymmetric flow. [This result is generally valid for a monotonically varying density law, as evident from (79b).]

Equations (81) and (82) can be used to define an equivalent relaxation time τ implicitly in terms of the stagnation-point pressure, even if relation (80) is a

poor approximation. Such τ would in general be different for plane and axisymmetric flow. A more common way to define yet another equivalent τ is in terms of the stand-off distance, as given by equation (A 4) of the appendix for axisymmetric flow. The numerical calculations presented in table 1 of Conti & Van Dyke (1969*a*) for dissociation of a Lighthill gas provide an illustration. For the value of their non-dimensionless reaction-rate constant

$$\bar{\Gamma} \equiv -\Gamma \rho_s R_s / v_s = 1{\cdot}3899 \times 10^5,$$

the pressure data corresponds to $\Lambda = 6{\cdot}8$ for axisymmetric flow and $\Lambda = 5$ for plane flow, while the detachment distance yields $\Lambda = 3{\cdot}5$. Another test of the validity of relation (80) is to examine the variation of the ratio $\bar{\Gamma}/\Lambda$ (which should be constant) with $\bar{\Gamma}$ (based on either pressure or detachment distance). The data for axisymmetric flow reveals a marked variation over the range of $\bar{\Gamma}$ presented, which is more pronounced with Λ determined by the pressure than that determined by the detachment distance. An examination of the (unpublished) density distribution on the axis does show a marked departure from the linear relaxation model (80). This is not surprising, since dissociation predominates at early times, while recombination becomes equally important as equilibrium is approached. The two processes influence the density law in different ways, both highly non-linear. A generalization of relation (80) that may be used to characterize these more complex distributions is the multiple relaxation model of the form

$$\bar{\rho}_{ns}^{-1}(t) = \epsilon_e + (\epsilon_f - \epsilon_e)\left(\sum_n a_n e^{-t/\tau_n}\right); \quad \sum_n a_n = 1. \tag{84}$$

This is equivalent to assuming n successive relaxation processes and requires the specification of $2n-1$ constants. The results for the stagnation pressure are then

$$\frac{\bar{p}_b - \bar{p}_{bf}}{\bar{p}_{be} - \bar{p}_{bf}} = 1 - 2(1+j)\left[\sum_n a_n e^{\Lambda_n} E_{3+2j}(\Lambda_n)\right], \tag{85a}$$

$$= \sum_n a_n \Lambda_n e^{\Lambda_n} E_{2(1+j)}(\Lambda_n), \tag{85b}$$

where

$$\Lambda_n = R_s / U_\infty \tau_n. \tag{86}$$

The above analysis shows that the relevant geometric parameter that determines the stagnation-point conditions is the shock radius R_s, independent of the shape of the body. In practice, however, it is some characteristic length L of a particular body shape that is known. A method of determining the relation between L and R_s is discussed in the appendix.

7. Concluding remarks

We have found that for finite relaxation times, the stagnation-point state is always in equilibrium, lying very close to the state given by equilibrium flow. The state given by identically frozen flow (infinite relaxation times) is in general far removed from these equilibrium states (except for the enthalpy and pressure). For certain state variables, the stagnation-point value for non-equilibrium flow may not be bounded by the values given by equilibrium and frozen flows.

The stagnation-point variable experiencing the greatest sensitivity to changes in non-equilibrium conditions is the pressure. Fortunately, the pressure is unaffected by the molecular transport processes, such as viscosity, heat conduction, and diffusion, which are all present in a real flow. This suggests that an accurate measurement of the stagnation-point pressure can be used to obtain information about relaxation times for simple non-equilibrium processes. Such a procedure would be an alternative to those based on the stand-off distance (Wegener & Buzyna 1969) when flow visualization is not feasible.

The results of this paper are only valid for blunt-nosed bodies. Sharp-nosed bodies (that still support a detached shock wave) have a velocity field in the neighbourhood of the apex that varies as a fractional power of the distance. A fluid particle thus requires only a finite time to reach the stagnation point. In this case, the complete range of conditions from equilibrium to identically frozen flow are attainable at the stagnation point.

The inclusion of molecular transport processes will naturally alter the results of this paper, particularly in the near-frozen régime. The inviscid analysis presented here is still a necessary first step in the solution of the complete problem. Such a solution has recently been carried out by Conti & Van Dyke (1969*b*).

The author is indebted to R. J. Conti and W. G. Vincenti for many helpful discussions.

Appendix. Stand-off distance in non-equilibrium flows

The variation of the shock stand-off distance δ with the non-equilibrium processes is important in certain experimental studies of non-equilibrium flow. It also plays a role in relating the body geometry to the shock radius, as will be shown below.

The ratio δ/R_s for axisymmetric flow is obtained directly by combining equations (16), (72) and (76) to yield

$$\delta/R_s \approx \frac{U_\infty}{R_s}\int_0^\infty \frac{1}{\bar{\rho}_{ns}(t)}\left(1+\frac{tU_\infty}{R_s}\right)^{-2} dt. \tag{A 1}$$

In the limits of equilibrium and frozen flows one obtains

$$(\delta/R_s)_e \approx \epsilon_e, \tag{A 2a}$$

and

$$(\delta/R_s)_f \simeq \epsilon_f. \tag{A 2b}$$

The normalized stand-off function then becomes

$$F[R_s;\bar{\rho}_{ns}(t)] \equiv \frac{\delta/R_s-(\delta/R_s)_e}{(\delta/R_s)_f-(\delta/R_s)_e} = \frac{\dfrac{U_\infty}{R_s}\displaystyle\int_0^\infty \frac{1}{\bar{\rho}_{ns}(t)}\left(1+\frac{tU_\infty}{R_s}\right)^{-2} dt-\epsilon_e}{\epsilon_f-\epsilon_e}. \tag{A 3}$$

For the linear relaxation model (80) this reduces to the relation first derived by Blythe (1963),

$$F(\Lambda) = e^\Lambda E_2(\Lambda) = 1-\Lambda e^\Lambda E_1(\Lambda). \tag{A 4}$$

Equations (A 3) and (A 4) should be highly accurate if the exact values of $(\delta/R_s)_f$ and $(\delta/R_s)_e$ obtained from numerical solutions are used.

For plane flows, the use of (76) leads to an infinite stand-off distance. Following Murzinov (1961), we replace the right-hand side of (13*b*) by a constant, so that (74) is replaced by

$$\frac{d}{d\bar{t}}(\bar{u}_{\bar{x}}) + \bar{u}_{\bar{x}}^2 \approx C; \quad \bar{u}_{\bar{x}}(0) \approx 1, \tag{A 5}$$

where C is a constant of order ϵ.

The solution of (A 5), when substituted into (13*a*) yields the following relation for $\bar{\rho}\bar{v}$:

$$\bar{\rho}\bar{v} \approx -\frac{\sinh C^{\frac{1}{2}}}{\sinh [C^{\frac{1}{2}}(1+\bar{t})]}, \tag{A 6}$$

where we have used the approximation $\tanh^{-1} C^{\frac{1}{2}} \approx C^{\frac{1}{2}}$. The quantity C is not truly a constant, since it should be proportional to ϵ_e for equilibrium flow, and ϵ_f for frozen flow. This suggests replacing C by a term proportional to $\bar{\rho}_{ns}^{-1}(t)$. Choosing the proportionality constant so as to yield the correct expressions for stand-off distance (to lowest order in ϵ) in the limits of equilibrium and frozen flow, we obtain as our final expression

$$\bar{\rho}\bar{v}(t) \approx \frac{-\sinh (3/\bar{\rho}_{ns}(t))^{\frac{1}{2}}}{\sinh [(3/\bar{\rho}_{ns}(t))^{\frac{1}{2}}(1+(tU_\infty/R_s))]}. \tag{A 7}$$

Using (A 7), we obtain for the normalized stand-off distance in plane flow the expression

$$F[R_s; \bar{\rho}_{ns}(t)] = \frac{\dfrac{U_\infty}{R_s}\displaystyle\int_0^\infty \frac{\sinh (3/\bar{\rho}_{ns}(t))^{\frac{1}{2}}\, dt}{\bar{\rho}_{ns}(t) \sinh \{(3/\bar{\rho}_{ns}(t))^{\frac{1}{2}}[1+(tU_\infty/R_s)]\}} - f(\epsilon_e)}{f(\epsilon_f) - f(\epsilon_e)}, \tag{A 8}$$

where

$$f(\epsilon) = (\tfrac{1}{3}\epsilon)^{\frac{1}{2}} \sinh (3\epsilon)^{\frac{1}{2}} \log|\operatorname{cotanh}(\tfrac{3}{4}\epsilon)^{\frac{1}{2}}|. \tag{A 9}$$

To lowest order in ϵ,

$$f(\epsilon) \approx \tfrac{1}{2}\epsilon \log(4/3\epsilon),$$

which agrees with the constant-density solution for δ/R_s in plane flow (Hayes & Probstein 1966).

In order to relate the body geometry to the shock geometry, the ratio δ/L is required, where L is some characteristic length of the particular body shape. A reasonable assumption for the variation of δ/L is

$$\frac{(\delta/L) - (\delta/L)_e}{(\delta/L)_f - (\delta/L)_e} \approx F(R_s). \tag{A 10}$$

Combining (A 10) with the definition of $F(R_s)$ we obtain

$$\frac{L}{R_s} = \frac{[(\delta/R_s)_f - (\delta/R_s)_e]F(R_s) + (\delta/R_s)_e}{[(\delta/L)_f - (\delta/L)_e]F(R_s) + (\delta/L)_e}, \tag{A 11}$$

where $F(R_s)$ is given by (A 3) for axisymmetric flow, and (A 8) for plane flow. The other quantities on the right-hand side of (A 11) are obtained from exact numerical solutions.

Relation (A 11) is most important when the body shape departs markedly from that of a sphere (or circular cylinder), so that ($L \not\approx R_s$). Under these conditions, assumption (A 10) is also the most suspect. As an extreme example, we consider

axisymmetric flow past a flat-faced cylinder, for which L is the cylindrical radius. For this case,

$$\left(\frac{\delta}{L}\right)_f = a\epsilon_f^{\frac{1}{2}}; \quad \left(\frac{\delta}{L}\right)_e = a\epsilon_e^{\frac{1}{2}}, \tag{A 12}$$

where a is a constant (Hayes & Probstein 1966). If we assume that $\delta/L = a(\delta/R_s)^{\frac{1}{2}}$ over the whole range of non-equilibrium conditions [as suggested by equations (A 2) and (A 12)], we can easily calculate the maximum error in L/R_s as given by (A 11). It is found to occur at $\delta/R_s = (\epsilon_e\epsilon_f)^{\frac{1}{2}}$, and gives for the ratio of the exact to the approximate value the relation

$$\frac{L/R_s}{(L/R_s)_{\text{approx}}} = \frac{2(\epsilon_f/\epsilon_e)^{\frac{1}{4}}}{1+(\epsilon_f/\epsilon_e)^{\frac{1}{2}}}. \tag{A 13}$$

A reasonable value for the maximum value of ϵ_f/ϵ_e attainable in practice is 4. Substituting in (A 13) one finds a ratio of 0·94. Thus, the use of (A 11) to estimate R_s in terms of the body geometry will lead to at most a 6 % error under the most extreme conditions. Since the normalized pressure has a logarithmic dependence on R_s, as shown by figure 2, this would correspond to a negligible uncertainty in the prediction of the pressure. Thus, (A 11) is a useful approximation for all body shapes and non-equilibrium flow conditions.

REFERENCES

Anisimov, S. I. & Khodyko, Yu. V. 1964 *Soviet Physics-Technical Physics* (*Zh. Tekhn. Fiz.*), **8**, 993.

Belotserkovskii, O. M. 1966 *Supersonic Gas Flow Around Blunt Bodies* (*Theoretical and Experimental Investigations*). Vychislitel'nyi Tsentr Akad. Nauk SSSR, Moscow. *NASA Tech. Transl.* no. F–453 (1967).

Belotserkovskii, O. M. & Dushin, V. K. 1964 *Zh. Vych. Mat. i Matem. Fiz.* **4**, 61. Transl. in *U.S.S.R. Comput. Math. and Math. Phys.* **4**, no. 1, 83.

Blythe, P. A. 1963 *Aero. Quart.* **14**, 357.

Chisnell, R. F. 1966 *AIAA J.* **4**, 1848.

Conti, R. J. 1964 *AIAA J.* **2**, 2044.

Conti, R. J. 1966 *J. Fluid Mech.* **24**, 65.

Conti, R. J. & Van Dyke, M. D. 1966 *Abstracts of Papers*, 1966 *Divisional Meeting of the Division of Fluid Dynamics, American Physical Society.*

Conti, R. J. & Van Dyke, M. 1969*a* *J. Fluid Mech.* **35**, 799.

Conti, R. J. & Van Dyke, M. 1969*b* *J. Fluid Mech.* **38**, 513.

Dushin, V. K. & Lun'kin, Yu. P. 1966 *Soviet Physics–Technical Physics* (*Zh. Tekhn. Fiz.*), **10**, 1133.

Emanuel, G. 1963 *Arnold Engr. Devel. Center*, AEDC-TDR-63-82.

Freeman, N. C. 1958 *J. Fluid Mech.* **4**, 407.

Gibson, W. E. & Marrone, P. V. 1962*a* *Phys. Fluids*, **5**, 1649.

Gibson, W. E. & Marrone, P. V. 1962*b* *AGARD N.A.T.O. Specialists Meeting on High Temperature Aspects of Hypersonic Flow*, Brussels (Preprint only).

Gibson, W. E. & Marrone, P. V. 1962*c* *Cornell Aero. Lab. Rep.* no. QM-1626-A-8.

Gilinskiy, S. M., Telenin, G. F. & Tinyakov, G. P. 1964 *Izv. Akad. Nauk SSR., Mech. i Mashinostr*, no. 4, 9. *NASA Tech. Transl.* no. F-297 (1965).

Hayes, D. H. & Probstein, R. F. 1966 *Hypersonic Flow Theory*, vol. I. New York: Academic.

HERMANN, R. 1965 *Univ. of Alabama Res. Inst. Rep.* no. 30.

LICK, W. 1960 *J. Fluid Mech.* **7**, 128.

LUN'KIN, YU. P. & POPOV, F. D. 1964 *Zh. Vych. Mat. i Matem. Fiz.* **4**, 896. Transl. in *U.S.S.R. Comput. Math and Math. Phys.* **4**, no. 5, 145.

LUN'KIN, YU. P. & POPOV, F. D. 1966 *Soviet Physics—Technical Physics* (*Zh. Tekhn. Fiz.*), **11**, 491.

LUN'KIN, YU. P. & SHTENGEL, M. P. 1964 *Politekh. Inst. Trudy Leningrad*, **230**, 7. Transl. as *Tech. Rep.* no. FTD-TT-65-649/1+2+4, Wright-Patterson Air Force Base, Ohio (1965).

MOECKEL, W. E. & WESTON, K. C. 1958 *NASA TN* 4265.

MURZINOV, I. N. 1961 *Izv. Akad. Nauk SSSR, Mekh. i Mashinostr.* no. 6, 33. Transl. as *Tech. Rep.* no. FTD-TT-62-1313-1+2+4, Wright-Patterson Air Force Base, Ohio (1962).

SAIAPIN, G. N. 1966 *Izv. AN SSR, Mekh. Zhidk. i Gaza*, no. 6, 115. Transl. by M. D. Friedman, available from Center for Scientific and Technical Information, Dept. of Comm., Springfield, Virginia.

SANDERS, R. W. 1958 *Lockheed Missiles and Space Company Rep.* no. IAD-351.

SHIH, W. C. L. & BARON, J. R. 1964 *AIAA J.* **2**, 1062.

STULOV, V. P. & TELENIN, G. F. 1965 *Izv. AN SSSR, Otd. Tekhn. Nauk, Mekhanika*, no. 1, 3. Transl. by M. D. Friedman, available from Center for Scientific and Technical Information, Dept. of Comm., Springfield, Virginia.

STULOV, V. P. & TURCHAK, L. I. 1966 *Izv. AN SSSR, Mekh, Zhidk. i Gaza*, no. 5, 3. Transl. by M. D. Friedman, available from Center for Scientific and Technical Information, Dept. of Comm., Springfield, Virginia.

SWIGART, R. J. 1963 *AIAA J.* **1**, 1034.

USTINOV, M. D. 1960 *Inzh. sborn.* **29**, 119.

VINCENTI, W. G. & KRUGER, C. H. 1965 *Introduction of Physical Gas Dynamics.* New York: Wiley.

WEGENER, P. P. & BUZYNA, G. 1969 *J. Fluid Mech.* **37**, 325.